

Chemotherapy-triggered cathepsin B release in myeloid-derived suppressor cells activates the Nlrp3 inflammasome and promotes tumor growth

Mélanie Bruchard^{1,2,8}, Grégoire Mignot^{1,2,8}, Valentin Derangère^{1,2}, Fanny Chalmin^{1,2}, Angélique Chevriaux¹⁻³, Frédérique Végran^{1,2}, Wilfrid Boireau⁴, Benoit Simon⁴, Bernhard Ryffel⁵, Jean Louis Connat⁶, Jean Kanellopoulos⁷, François Martin^{1,2}, Cédric Rébé¹⁻³, Lionel Apetoh^{1-3,8} & François Ghiringhelli^{1-3,8}

Chemotherapeutic agents are widely used for cancer treatment. In addition to their direct cytotoxic effects, these agents harness the host's immune system, which contributes to their antitumor activity. Here we show that two clinically used chemotherapeutic agents, gemcitabine (Gem) and 5-fluorouracil (5FU), activate the NOD-like receptor family, pyrin domain containing-3 protein (Nlrp3)-dependent caspase-1 activation complex (termed the inflammasome) in myeloid-derived suppressor cells (MDSCs), leading to production of interleukin-1 β (IL-1 β), which curtails anticancer immunity. Chemotherapy-triggered IL-1 β secretion relied on lysosomal permeabilization and the release of cathepsin B, which bound to Nlrp3 and drove caspase-1 activation. MDSC-derived IL-1 β induced secretion of IL-17 by CD4⁺ T cells, which blunted the anticancer efficacy of the chemotherapy. Accordingly, Gem and 5FU exerted higher antitumor effects when tumors were established in *Nlrp3*^{-/-} or *Casp1*^{-/-} mice or wild-type mice treated with interleukin-1 receptor antagonist (IL-1Ra). Altogether, these results identify how activation of the Nlrp3 inflammasome in MDSCs by 5FU and Gem limits the antitumor efficacy of these chemotherapeutic agents.

Immune responses against cancer are an important factor determining tumor evolution^{1,2}. In many experimental and human cancers, T cell immune responses are involved in tumor-growth control and restrain tumor progression. By contrast, the role of cytotoxic agents on immune responses remains largely unresolved. Chemotherapy treatment in cancer has long been suspected to induce systemic immunosuppression³. However, recent studies report that some chemotherapeutic agents instead enhance antitumor immune responses through their capacity to eliminate immunosuppressive cells or trigger 'immunogenic cell death' of tumor cells^{4,5}. Two drugs, Gem⁶⁻⁸ and 5FU⁹, selectively deplete MDSCs⁹⁻¹¹, a population of immature myeloid cells that suppresses T cell activation in humans and mice¹²⁻¹⁴. 5FU-mediated MDSC depletion increased interferon- γ (IFN- γ) production by tumor-specific CD8⁺ T cells and the survival of tumor-bearing mice but was insufficient to avoid tumor relapse, underscoring the need to identify additional molecular pathways that favor cancer-cell resistance to chemotherapy⁹.

Here we show that Gem and 5FU, in addition to their capacity to selectively kill MDSCs, activate the NLRP3 inflammasome in these cells, leading to IL-1 β release, which restrains their antitumor efficacy. Although IL-1 β did not affect the sensitivity of tumor cells to 5FU,

it enhanced the capacity of CD4⁺ T cells to produce IL-17, which limited the antitumor effect of 5FU through an IL-17-dependent proangiogenic effect. These results unravel the ambivalent effect of 5FU and Gem in the antitumor immune response.

RESULTS

5FU and Gem induce caspase-1 activation in MDSCs

We previously demonstrated that 5FU and Gem can induce cell death of MDSCs. Using MSC-2 cells, an established MDSC cell line⁹, we focused on the capacity of various chemotherapeutic agents to induce caspase-1 activation in MDSCs. We determined the drug concentrations that induced 50% MSC-2 cell death (Supplementary Fig. 1). Only Gem and 5FU activated caspase-1 in MDSCs (Fig. 1a). The dose effects of 5FU and Gem demonstrated that caspase-1 activation did not correlate with the amount of dead cells (Fig. 1b and Supplementary Fig. 2). We determined the kinetic activation of caspase-1 after 5FU treatment and showed that caspase-1 activation was detectable at around 12 h after 5FU treatment, meaning before evidence of cell death, which appears after 18 h (Fig. 1c). We found similar results using Gem (Supplementary Fig. 3). The delay in caspase-1 activation was expected, as both drugs require conversion

¹Institut National de la Santé et de la Recherche Médicale (INSERM) U866, Dijon, France. ²Faculté de Médecine et pharmacie, Université de Bourgogne, Dijon, France. ³Centre Georges François Leclerc, Dijon, France. ⁴Franche-Comté Electronique, Mécanique, Thermique et Optique-Sciences et Technologies (FEMTO-ST) Institute, Université de Franche Comté, Besançon, France. ⁵Laboratory of Molecular Immunology and Embryology, Centre National de la Recherche Scientifique (CNRS) Unités Mixtes de Recherche (UMR) 6218, Orléans, France. ⁶INSERM U866, Laboratoire de Physiopathologie et Pharmacologie Cardiovasculaires Expérimentales, Institut Fédérative de Recherche (IFR) Santé-Sciences et Techniques de l'Information et de la Communication (STIC), Faculté de Médecine, Université de Bourgogne, Dijon, France. ⁷UMR 8619, Université Paris Sud-Paris 11, Orsay Cedex, France. ⁸These authors contributed equally to this work. Correspondence should be addressed to F.G. (fghiringhelli@cgl.fr).

Received 20 July; accepted 17 October; published online 2 December 2012; doi:10.1038/nm.2999

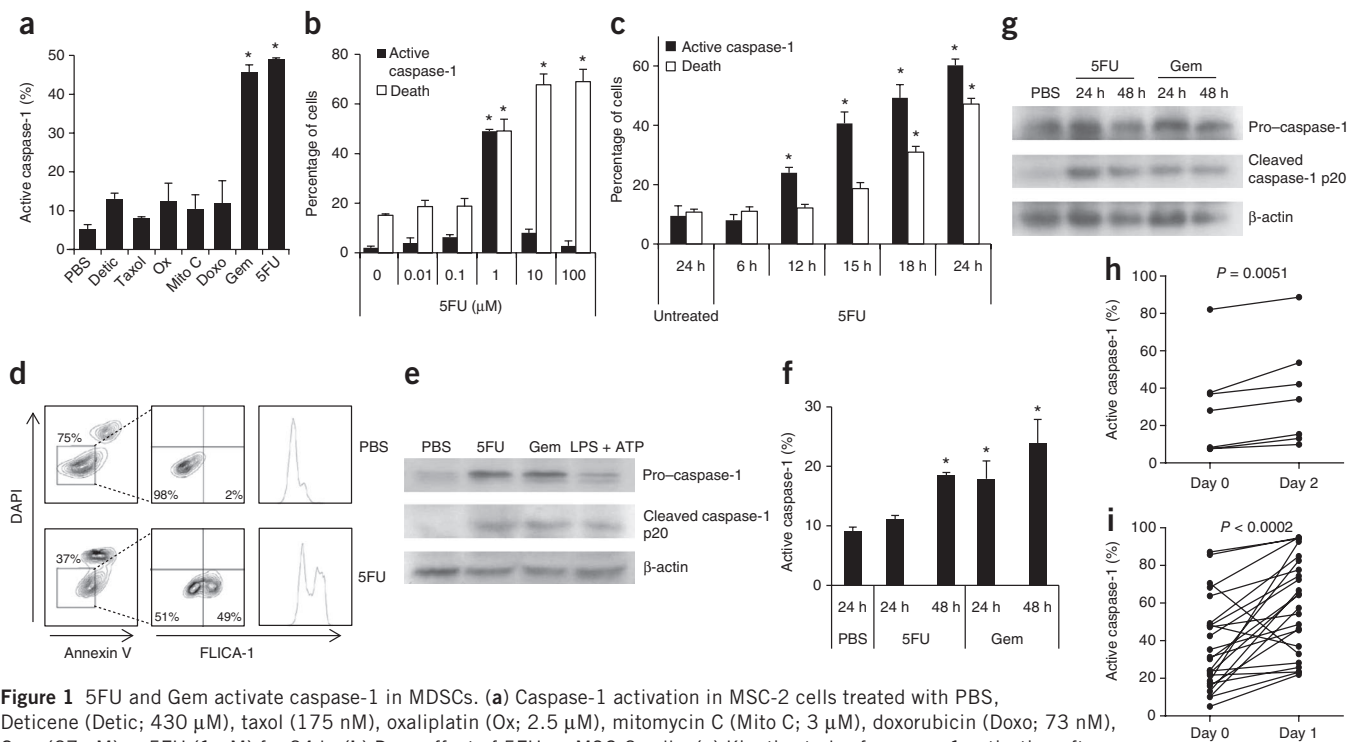


Figure 1 5FU and Gem activate caspase-1 in MDSCs. **(a)** Caspase-1 activation in MSC-2 cells treated with PBS, Deticene (Detic; 430 μM), taxol (175 nM), oxaliplatin (Ox; 2.5 μM), mitomycin C (Mito C; 3 μM), doxorubicin (Doxo; 73 nM), Gem (27 nM) or 5FU (1 μM) for 24 h. **(b)** Dose effect of 5FU on MSC-2 cells. **(c)** Kinetic study of caspase-1 activation after 5FU treatment (1 μM). In **a–c**, caspase-1 activation and cell death were measured using fluorescent probes and annexin V and DAPI staining, respectively. **(d)** DAPI and FLICA-1 fluorescence tested in MSC-2 cells treated with PBS or 5FU (1 μM) for 24 h. The percentages shown represent the frequency of positive cells. **(e)** Western blot detecting caspase-1 activation in MSC-2 cells treated with 5FU (1 μM), Gem (27 nM) or lipopolysaccharide (LPS) (100 ng ml^{-1}) and ATP (5 mM) as a positive control for 24 h. β -actin was used as a loading control. **(f,g)** Caspase-1 activation and cleaved caspase-1 in EL4 tumor-bearing mice treated with PBS, 5FU (50 mg per kg body weight) or Gem (120 mg per kg body weight). Caspase-1 activity after 24 h and 48 h in labeled splenic CD11b⁺Gr-1⁺ MDSCs **(f)**. Western blot detecting cleaved caspase-1 in sorted CD11b⁺Gr-1⁺ MDSCs **(g)**. **(h)** Caspase-1 activation, assessed by flow cytometry, in HLA DR⁺CD14⁺CD33⁺ MDSCs derived from PBMCs of patients with cancer that had been cultured with PBS or 5FU (1 μM) for 2 d. $n = 8$ patients. **(i)** Caspase-1 activation, assessed by fluorescent probe, in HLA DR⁺CD14⁺CD33⁺ MDSCs derived from PBMCs of patients with cancer obtained before and 1 d after *in vivo* 5FU treatment. $n = 24$ patients. Data are representative of one out of three experiments and are the mean \pm s.e.m. **(a–g)**. * $P < 0.05$ by Wilcoxon rank-sum test.

into an active metabolite^{15,16}. Notably, we found caspase-1 activation in live cells negative for both annexin V and DAPI (**Fig. 1d**). These data suggest that 5FU- and Gem-induced caspase-1 activation is dissociated from cell death. We confirmed these results using western blot (**Fig. 1e**). *In vitro*, 5FU induced caspase-1 activation in other myeloid subsets only at high doses that were not clinically relevant (100 μM) (**Supplementary Fig. 4**). *In vivo*, systemic treatment of tumor-bearing mice with Gem or 5FU induced activation of caspase-1 at 24 h or 48 h, respectively, in MDSCs (**Fig. 1f**), and the amount of caspase-1 activation was similar in monocytic and granulocytic MDSC subsets (**Supplementary Fig. 5**). Western blot analysis of cell-sorted splenic MDSCs confirmed this result (**Fig. 1g**). Kinetic analysis of splenic MDSC number and MDSC caspase-1 activation showed that caspase-1 activation occurred before the nadir of MDSC elimination (**Supplementary Fig. 6**).

In human MDSCs, we noted that 5FU activated caspase-1 in MDSCs from patients with metastatic colorectal cancer 48 h after *in vitro* administration (**Fig. 1h**). In addition, we also found caspase-1 activation in circulating MDSCs from 22 out of 24 patients with metastatic colorectal cancer who received chemotherapy containing 5FU ($P < 0.0002$) (**Fig. 1i**). We found similar caspase-1 activation in patients treated with 5FU plus oxaliplatin or irinotecan but not in patients treated without 5FU (data not shown). Double labeling using DAPI and caspase-1 fluorochrome inhibitor of caspase (FLICA) showed that 1 d after 5FU treatment the proportion of dying DAPI-positive cells

was unchanged and only the ratio of caspase-1-positive cells to living DAPI-negative cells increased, suggesting that 5FU induced caspase-1 activation in live cells rather than the death of caspase-1-negative MDSCs (**Supplementary Fig. 7**). Together these results demonstrate that 5FU and Gem activate caspase-1 in MDSCs *in vitro* and *in vivo*.

NLRP3-dependent induction of IL-1 β by 5FU and Gem

Caspase-1 activation is required for the secretion of bioactive IL-1 β ¹⁷. Accordingly, MDSCs from wild-type tumor-bearing mice treated with Gem or 5FU secreted IL-1 β (**Fig. 2a**). This IL-1 β secretion was comparable in both monocytic and granulocytic subsets (data not shown). MDSCs from tumor-bearing caspase-1-deficient (*Casp1*^{-/-}) mice treated with 5FU were unable to produce IL-1 β (**Fig. 2b**). These data suggest that 5FU and Gem activate caspase-1 in MDSCs, leading to IL-1 β secretion. *In vivo*, we found IL-1 β in the serum of tumor-bearing wild-type mice from day 2–10 after 5FU administration (**Fig. 2c**). Notably, MDSC depletion before 5FU treatment aborted IL-1 β production, suggesting that MDSCs are the primary producers of IL-1 β (**Supplementary Fig. 8**). In the cohort of patients with metastatic colorectal cancer who were treated with 5FU-based chemotherapy, IL-1 β serum concentrations were increased in 9 out of 12 patients 24 h after 5FU administration ($P = 0.03$) (**Fig. 2d**).

The NLRP3 inflammasome is frequently involved in caspase-1 activation induced by endogenous signals¹⁷. We found that *in vitro*

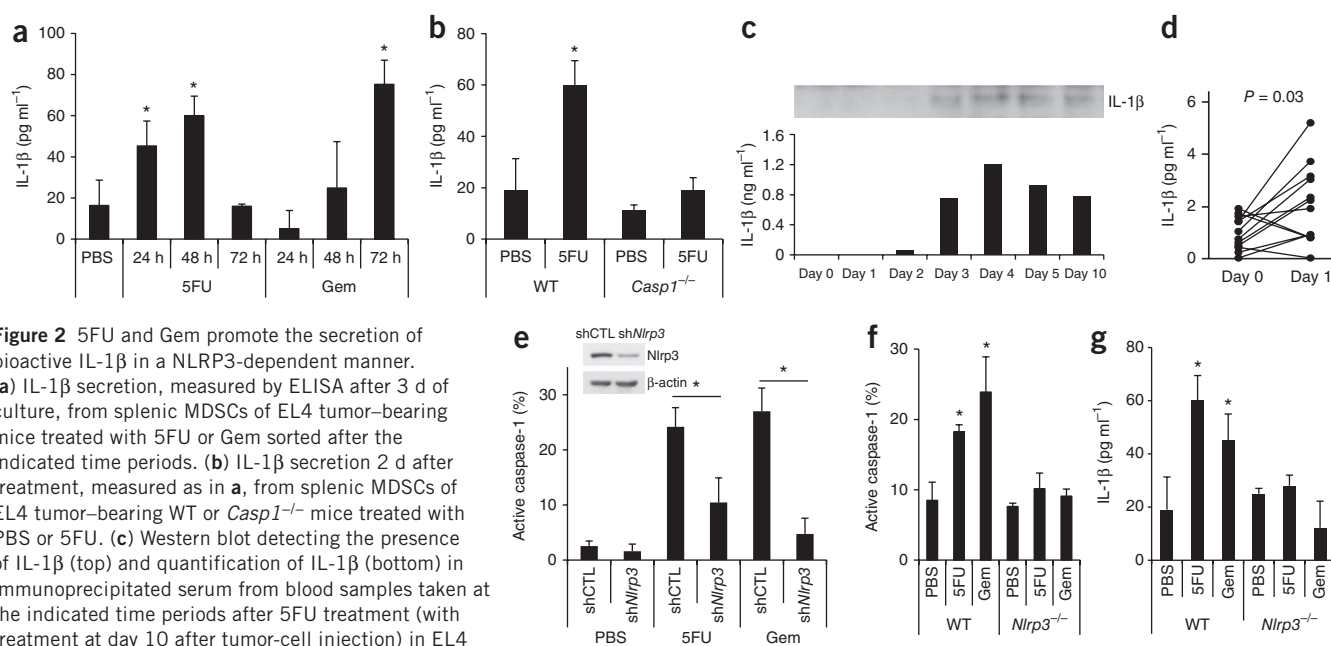


Figure 2 5FU and Gem promote the secretion of bioactive IL-1 β in a NLRP3-dependent manner. (a) IL-1 β secretion, measured by ELISA after 3 d of culture, from splenic MDSCs of EL4 tumor-bearing mice treated with 5FU or Gem sorted after the indicated time periods. (b) IL-1 β secretion 2 d after treatment, measured as in a, from splenic MDSCs of EL4 tumor-bearing WT or *Casp1*^{-/-} mice treated with PBS or 5FU. (c) Western blot detecting the presence of IL-1 β (top) and quantification of IL-1 β (bottom) in immunoprecipitated serum from blood samples taken at the indicated time periods after 5FU treatment (with treatment at day 10 after tumor-cell injection) in EL4 tumor-bearing mice. The serum was immunoprecipitated using IL-1 β -specific antibody. (d) IL-1 β concentration in the sera of patients with colon cancer obtained before and 1 d after *in vivo* 5FU treatment. $n = 12$ patients. (e) MSC-2 cells transduced with control shRNA (shCTL) or *Nlrp3* shRNA (sh*Nlrp3*) and treated with PBS, 5FU (1 μ M) or Gem (27 nM) for 24 h. Caspase-1 activation was measured by flow cytometry. Inset, NLRP3 expression in shCTL or sh*Nlrp3* using western blot. EL4 tumor-bearing WT or *Nlrp3*^{-/-} mice were treated with PBS, 5FU (50 mg per kg body weight) or Gem (120 mg per kg body weight). After 48 h, splenic CD11b⁺Gr-1⁺ cells were labeled. (f,g) Caspase-1 activation determined by flow cytometry (f) and IL-1 β secretion from sorted splenic MDSCs cultured for 3 days measured by ELISA (g). Data are representative of one out of five (a,e) or three (b,c,f,g) experiments and are the mean \pm s.e.m. * $P < 0.05$ by Wilcoxon rank-sum test.

treatment of MDSCs with Gem or 5FU activated caspase-1 in MDSCs transduced with control shRNA but not in those transduced with shRNA specific for *Nlrp3*, (Fig. 2e). In addition, 5FU and Gem activated caspase-1 in MDSCs from wild-type but not *Nlrp3*-deficient (*Nlrp3*^{-/-}) mice *in vivo* (Fig. 2f). MDSCs from tumor-bearing *Nlrp3*^{-/-} mice were also unable to produce IL-1 β after 5FU or Gem treatment, in contrast to wild-type mice (Fig. 2g). These data demonstrate that 5FU and Gem induce activation of the NLRP3 inflammasome in MDSCs, which triggers secretion of bioactive IL-1 β .

Cathepsin B mediates inflammasome activation

NLRP3 activation may occur through crystal phagocytosis, induction of radical oxygen species (ROS), altered calcium or potassium ionic movements, high concentrations of extracellular ATP or lysosome disruption and cathepsin B release¹⁸. To identify the NLRP3 activator in 5FU- and Gem-induced inflammasome activation, we tested the effect of selective inhibitors on caspase-1 activation in 5FU-treated MDSCs. 5FU-induced caspase-1 activation was not prevented by inhibition of phagocytosis, ROS synthesis or the P2X purinoceptor 7 (P2rx7) channel (Fig. 3a). Inhibition of lysosomal acidification using bafilomycin A blunted the caspase-1 activation induced by 5FU or Gem (Fig. 3a and data not shown). 5FU and Gem induced permeabilization of lysosomes (Fig. 3b). We detected mature cathepsin B in MDSCs treated with 5FU or Gem (Fig. 3c and Supplementary Fig. 9).

Moreover, we found reduced caspase-1 activation in MDSCs after 5FU or Gem treatment in the presence of a cathepsin B inhibitor¹⁹ or in MDSCs transfected with cathepsin B shRNA (Fig. 3d). Confocal microscopy confirmed that 5FU and Gem induced cathepsin B cytosolic release (Fig. 3e). In human MDSCs, caspase-1

activation induced by 5FU was blunted by the cathepsin B inhibitor (Fig. 3f). In a cohort of patients with metastatic colorectal cancer, we also observed that infusion of 5FU induced cathepsin B activity in circulating MDSCs in 16 of 21 patients ($P = 0.01$) (Fig. 3g). Together these data demonstrate that 5FU and Gem trigger NLRP3 inflammasome activation mainly through the release of cathepsin B in the cytosol as a result of chemotherapy-dependent lysosome permeabilization.

Cathepsin B directly interacts with Nlrp3

We found that mouse recombinant Nlrp3 and cathepsin B proteins co-precipitated *in vitro* (Fig. 4a). We confirmed the specificity of this interaction using human NLRP3 and cathepsin B recombinant proteins in a surface plasmon resonance assay (Fig. 4b).

In a cellular system, we also found a specific interaction between endogenous Nlrp3 and cathepsin B in mouse MSC-2 cells treated with 5FU (Fig. 4c). We obtained the same results with cell-sorted MDSCs from tumor-bearing mice, demonstrating that 5FU triggered this interaction in MDSCs (Fig. 4d). Nlrp3 contains three protein domains²⁰. We generated recombinant vesicular stomatitis virus (VSV)-tagged Nlrp3 protein deleted in the pyrin domain (PYD), the NACHT domain or the leucine-rich repeat (LRR) domain (Fig. 4e) and found that cathepsin B interacted with Nlrp3 deleted in the PYD or NACHT fragment but not with Nlrp3 deleted in the LRR fragment (Fig. 4f).

Cathepsin B was readily able to cleave the control protein nucleophosmin but not Nlrp3, suggesting that activation of Nlrp3 by cathepsin B is not caused by direct cleavage (Supplementary Fig. 10). Together, these data demonstrate that 5FU allows a direct interaction between cathepsin B and the LRR domain of Nlrp3 through release of cathepsin B from the lysosome.

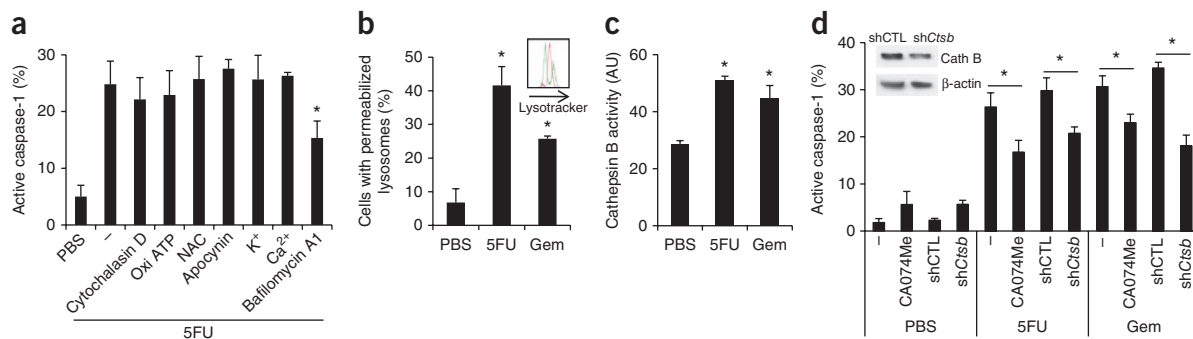


Figure 3 5FU- and Gem-induced NLRP3 inflammasome activation results from cathepsin B release from lysosomes.

(a) Caspase-1 activation, determined by flow cytometry, in MSC-2 cells treated with PBS or 5FU (1 μ M) in the absence or presence of cytochalasin D (200 nM), oxi ATP (150 μ M), *N*-acetylcysteine (NAC; 10 mM), apocynin (20 μ M) or bafilomycin A1 (10 nM) for 24 h or K^+ (140 mM) or Ca^{2+} (1.2 mM) for 1 h. (b) Lysosomal integrity, measured using LysoTracker, of MSC-2 cells treated with PBS, 5FU (1 μ M) or Gem (27 nM). The inset shows a representative LysoTracker signal (PBS-treated cells, red; 5FU-treated cells, green). (c) Cathepsin B activity, assessed by fluorometry, of the cells described in b. AU, arbitrary units. (d) Caspase-1 activation, determined as in a, in MSC-2 cells incubated in the absence or presence of the cathepsin B (Cath B) inhibitor CA074Me (33 μ M) or transduced with control shRNA (shCTL) or cathepsin B shRNA (sh*Ctsb*) and treated as in b. (e) Colocalization of cathepsin B and CD107a, assessed by confocal microscopy, in MSC-2 cells cultured on glass, treated for 24 h as in **Figure 2b** and fixed and stained for cathepsin B and CD107a. Scale bar, 10 μ m. (f) Caspase-1 activation, assessed by flow cytometry, in HLA DR⁺CD14⁺CD33⁺ MDSCs derived from PBMCs of patients with cancer that were cultured with PBS or 5FU (40 μ M) in the presence or absence of CA074Me for 2 d. (g) Cathepsin B activity, assessed by fluorometry, in PBMCs from patients with colon cancer obtained before and 1 d after *in vivo* 5FU treatment. Data are representative of one out of four experiments and are the mean \pm s.e.m. (a–e). * P < 0.05 by Wilcoxon rank-sum test.

IL-1 β production restrains 5FU antitumor effect
Genetic inactivation of *Nlrp3* or *Casp1* enhanced the antitumor efficacy of 5FU against EL4 thymoma growing *in vivo* (**Fig. 5a**). Whereas all wild-type mice died within 30 d, 42% and 30% of *Casp1*^{-/-} and *Nlrp3*^{-/-} mice, respectively, remained tumor free 60 d after 5FU treatment (**Supplementary Table 1**). Anakinra is a recombinant soluble IL-1Ra. Administration of anakinra enhanced the antitumor efficacy of 5FU in the EL4 tumor model and the combination induced cure in 45% of the mice (**Fig. 5b**). Notably, MDSC depletion before 5FU treatment aborted the antitumor effect of the IL-1Ra. Similarly, the enhanced efficacy of 5FU treatment in *Nlrp3*^{-/-} and *Casp1*^{-/-} mice was abrogated by MDSC depletion (**Supplementary Table 1**). We extended this observation to three other experimental tumor models: 4T1 mammary carcinoma, B16F10 melanoma and Lewis lung carcinoma (LLC) (**Fig. 5c**).

IL-1 β production restrains 5FU antitumor effect

We noted that neither IL-1 β nor IL-1Ra had an impact on the direct cytotoxic effect of 5FU in the EL4, B16, LLC or 4T1 tumor cell models (**Fig. 5d** and **Supplementary Fig. 11**). In addition, genetic inactivation of IL-1R markedly enhanced the antitumor efficacy of 5FU against EL4 thymomas *in vivo*, thus demonstrating that IL-1 β does not exert its effect on tumor cells but rather on host cells (**Fig. 5e**).

We noted that neither IL-1 β nor IL-1Ra had an impact on the direct cytotoxic effect of 5FU in the EL4, B16, LLC or 4T1 tumor cell models (**Fig. 5d** and **Supplementary Fig. 11**). In addition, genetic inactivation of IL-1R markedly enhanced the antitumor efficacy of 5FU against EL4 thymomas *in vivo*, thus demonstrating that IL-1 β does not exert its effect on tumor cells but rather on host cells (**Fig. 5e**).

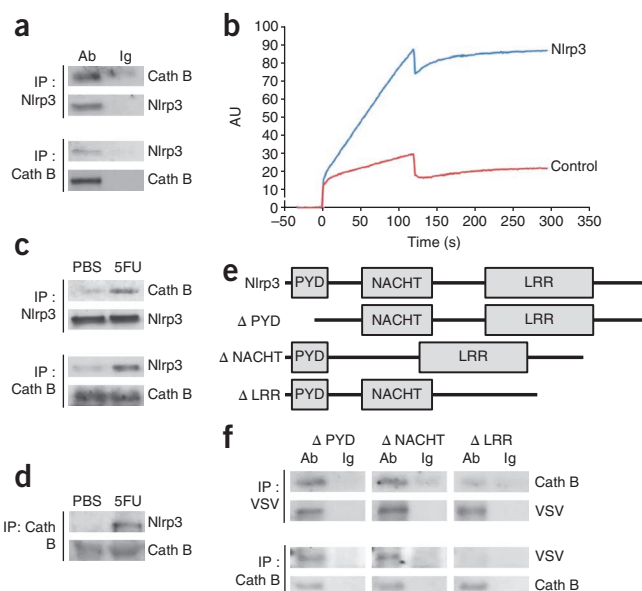
IL-1 β production enhances IL-17 production by CD4⁺ T cells

IL-1 β has a crucial role in inflammation²¹, as illustrated by its ability to induce IL-17 secretion from proinflammatory CD4⁺ T cells^{22,23}. IL-1 β has also been implicated in CD8⁺ T cell activation⁵. We found that although high concentrations of IL-1 β were required for activating

CD8⁺ T cells (**Supplementary Fig. 12**), low concentrations of IL-1 β , similar to those released by MDSCs as a result of 5FU treatment, were sufficient to trigger IL-17 production by CD4⁺ cells (**Fig. 6a**) but did not induce production of IFN- γ or IL-4, expression of forkhead box P3 (Foxp3) or activation of CD8⁺ T cells (data not shown). Notably, CD4 depletion enhanced the antitumor effect of 5FU but did not improve the effect of the combination of 5FU plus IL-1Ra, suggesting that CD4⁺ T cells limit 5FU efficacy in an IL-1-dependent manner (**Fig. 6b**). In contrast, CD8⁺ T cell depletion had no impact on the antitumor efficacy of 5FU or 5FU plus IL-1Ra (**Supplementary Fig. 13**).

We found that naive T cells cultured with MDSCs isolated from tumor-bearing mice treated with Gem or 5FU differentiated into IL-17-producing CD4⁺ T cells in an IL-1-dependent manner (**Fig. 6c**). To validate the involvement of the NLRP3 inflammasome in IL-17 secretion from CD4⁺ T cells, we cultured naive T cells with MDSCs from tumor-bearing wild-type, *Casp1*^{-/-}, *Nlrp3*^{-/-}, cathepsin B-deficient (*Ctsb*^{-/-}) or *P2rx7*^{-/-} (control) mice treated with or without 5FU. We found that only wild-type or control *P2rx7*^{-/-} MDSCs from tumor-bearing mice treated with 5FU were able to enhance IL-17 production by CD4⁺ T cells in an IL-1-dependent manner, whereas *Casp1*^{-/-}, *Nlrp3*^{-/-} and *Ctsb*^{-/-} MDSCs were unable to do so (**Fig. 6c**). We confirmed these results using ROR- γ t-GFP mice (**Supplementary Fig. 14**). *In vivo*, 5FU and Gem enhanced the capacity of CD4⁺ cells in tumor-draining lymph nodes to produce IL-17 in a caspase-1-dependent manner; however, caspase-1 deficiency did not affect IL-4 or IFN- γ secretion by these cells (**Fig. 6d** and data not shown).

Figure 4 Nlrp3 binds to cathepsin B. **(a)** Immunoprecipitation (IP) and western blot performed using antibodies to Nlrp3 or cathepsin B (Ab) or isotype control antibodies (Ig). Recombinant mouse Nlrp3 protein synthesized *in vitro* using a cell-free system and incubated with recombinant mouse cathepsin B (Cath B) for 1 h before immunoprecipitation. **(b)** Surface plasmon resonance studying the binding of Nlrp3 (10 nM) to a cathepsin B protein chip and a rat albumin serum (RSA) control chip. **(c)** Immunoprecipitation and western blots performed as in **a** of MSC-2 cells treated with PBS or 5FU (1 μ M) for 24 h. **(d)** Immunoprecipitation performed with antibody to cathepsin B followed by western blot performed with antibody to Nlrp3 of cell-sorted splenic MDSCs from EL4 tumor-bearing mice 24 h after treatment with PBS or 5FU (50 mg per kg body weight). **(e)** The design of VSV-tagged recombinant mouse Nlrp3 deleted (Δ) in the PYD or the NACHT or LRR domain. **(f)** Immunoprecipitation and western blot performed as in **a** on the truncated Nlrp3 proteins described in **e** and incubated with recombinant mouse cathepsin B. Data are representative of one out of three experiments (**a**–**f**).



We also found an increased frequency of CD4⁺GFP⁺ cells in the tumor-draining lymph nodes of ROR- γ T-GFP mice after treatment with Gem or 5FU. This increase was abrogated by IL-1Ra injection (**Supplementary Fig. 15**). In humans, we found enhanced production of IL-17 in peripheral blood mononuclear cells (PBMCs) 14 d after 5FU treatment (**Fig. 6e**).

IL-17 has been reported to promote angiogenesis^{24–26}, resulting in tumor progression. In mice, we found that *in vivo* 5FU drove the expression of T helper type 17 (T_H17) cell-related genes (*Il17a* and *Rorc*) in the tumor bed, as well as the expression of angiogenesis-related genes (*Eng* and *Pecam1*), whereas we did not observe increased expression of these genes when we used 5FU plus IL-1Ra (**Fig. 6f**).

As MDSC-derived IL-1 β enhanced IL-17 secretion from CD4⁺ T cells, we tested whether the enhanced antitumor effect between 5FU and the inhibition of IL-1 β relied on downregulation of IL-17. 5FU showed a better antitumor efficacy in *Il17a*^{-/-} mice compared to its effect in wild-type mice (**Fig. 6g**), and IL-1Ra did not enhance the efficacy of 5FU in *Il17a*^{-/-} mice (**Fig. 6g**). Together these data demonstrate that 5FU drives IL-1-dependent CD4⁺ T cell polarization into IL-17-producing cells and IL-17 limits the therapeutic effect of 5FU.

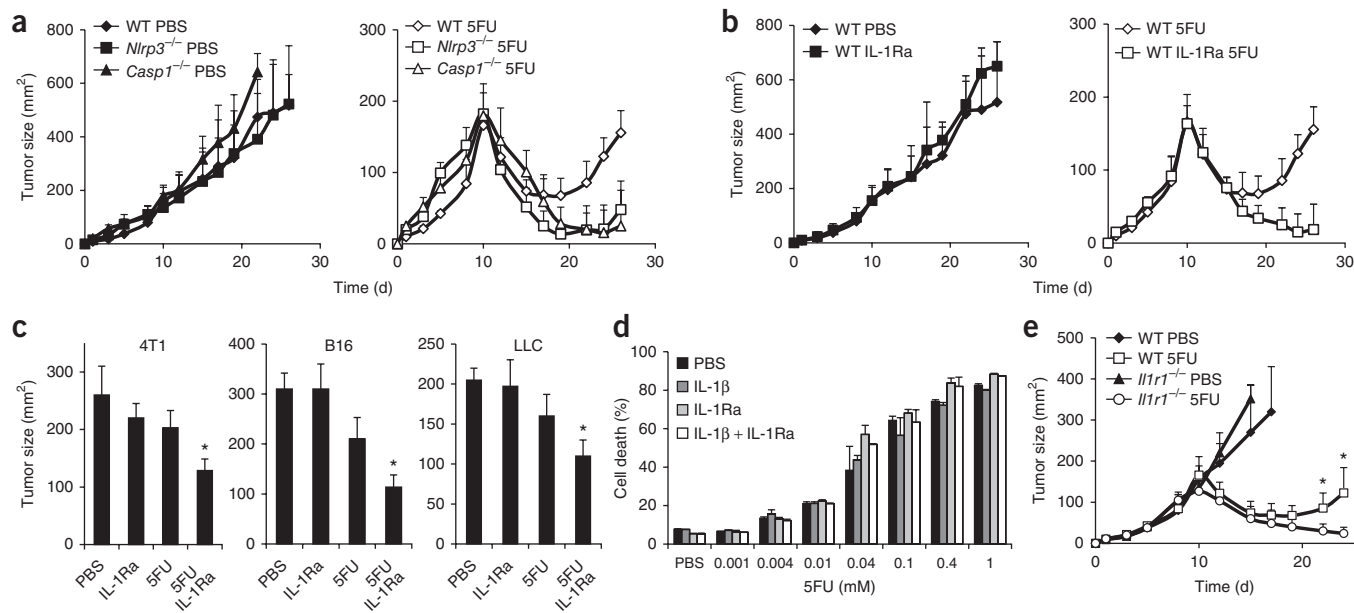
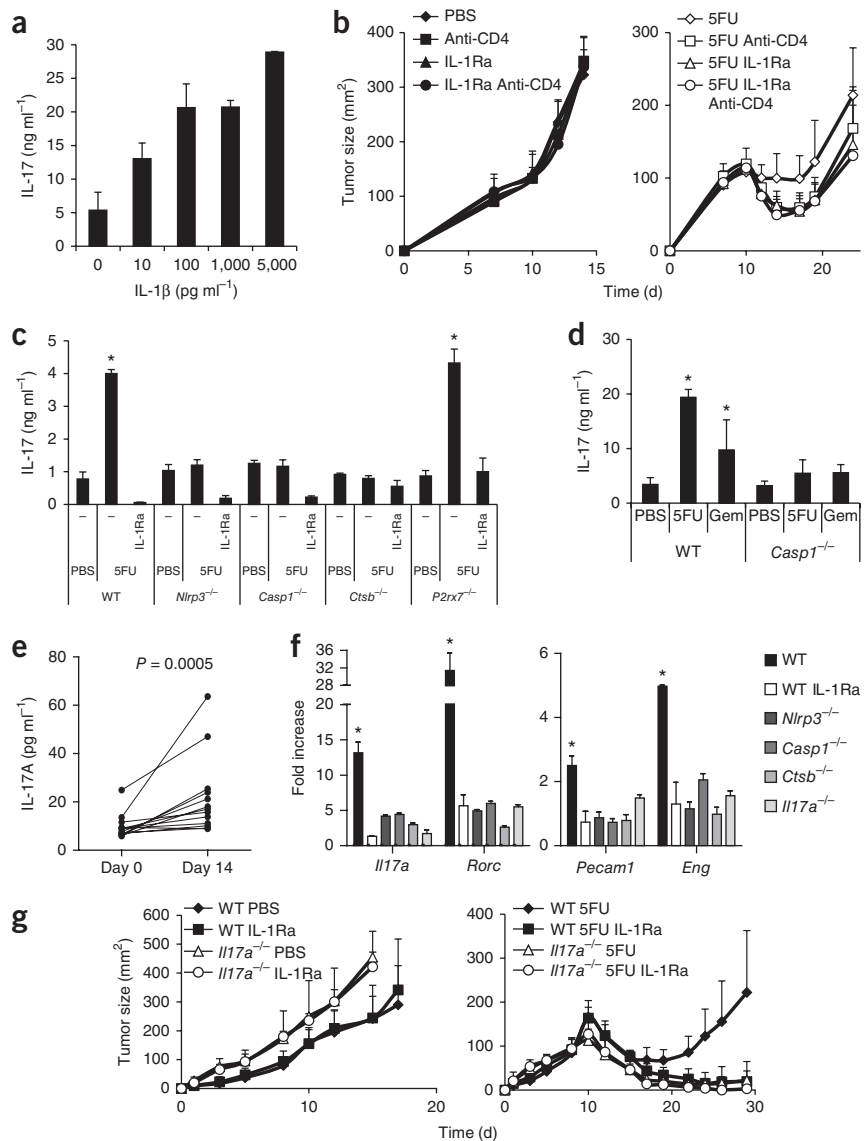


Figure 5 NLRP3-dependent IL-1 β production restrains the antitumor effect of 5FU. **(a)** Tumor growth, monitored three times a week, in EL4 tumor-bearing WT, *Nlrp3*^{-/-} and *Casp1*^{-/-} mice that received PBS (left) or 5FU (50 mg per kg body weight; right) 10 d after tumor-cell injection. **(b)** Tumor growth, monitored as in **a**, in EL4 tumor-bearing WT mice treated with PBS or IL-1Ra (1.5 mg per kg body weight) three times a week that also received PBS (left) or 5FU (50 mg per kg body weight; right) 10 d after tumor-cell injection. **(c)** Tumor growth, monitored as in **a**, in WT mice with 4T1, B16 or LLC tumors treated with PBS or IL-1Ra (1.5 mg per kg body weight) three times a week that also received PBS or 5FU (50 mg per kg body weight) at days 5 and 7 (4T1 and LLC) or days 5, 7 and 9 (B16). Tumor sizes at days 20 (4T1), 18 (B16) and 30 (LLC) are shown. **(d)** Viability of EL4 cells treated with increasing doses of 5FU alone or with IL-1 β (200 pg ml⁻¹), IL-1Ra (10 nM) or both assessed after 2 d by flow cytometry. **(e)** As described in **a** but using *Il1r1*^{-/-} and WT mice. Data are representative of one out of three experiments and are the mean \pm s.e.m. (**a**–**e**).

* $P < 0.05$ by Wilcoxon rank-sum test.

Figure 6 NLRP3-dependent IL-1 β production enhances IL-17 production by CD4 $^{+}$ T cells that restrain the antitumor effect of 5FU.

(a) IL-17 concentrations, assessed by ELISA, in IL-17-secreting T cells generated from purified naive CD4 $^{+}$ CD62L $^{+}$ T cells that were stimulated with antibodies to CD3 and CD28 along with TGF- β , IL-6 and increasing doses of IL-1 β for 72 h. (b) Tumor growth in EL4 tumor-bearing WT mice depleted of CD4 $^{+}$ T cells and treated as in **Figure 5b**. (c) IL-17 secretion, measured after 3 d by ELISA, in splenic MDSCs from EL4 tumor-bearing WT, *Nlrp3* $^{-/-}$, *Casp1* $^{-/-}$, *Ctsb* $^{-/-}$ or *P2rx7* $^{-/-}$ mice treated with PBS or 5FU (50 mg per kg body weight) that were cultured after 48 h with naive CD4 $^{+}$ CD62L $^{+}$ T cells and activated in the presence of antibodies to CD3 (5 μ g ml $^{-1}$) and CD28 (5 μ g ml $^{-1}$) in the absence or presence of IL-1Ra (10 nM). (d) IL-17 secretion, measured after 3 d by ELISA, in draining lymph node cells harvested after 5 d from EL4 tumor-bearing WT or *Casp1* $^{-/-}$ mice treated with PBS, 5FU (50 mg per kg body weight) or Gem (120 mg per kg body weight) and activated in the presence of antibodies to CD3 (5 μ g ml $^{-1}$) and CD28 (5 μ g ml $^{-1}$). (e) IL-17A production, measured by ELISA after stimulation with monoclonal antibodies to CD3 and CD28, in PBMCs from 13 patients with colon cancer obtained before and 14 d after *in vivo* 5FU treatment. (f) Quantitative real-time PCR after 48 h measuring the expression of *Il17a* and *Rorc* (relative to the expression of *Cd3e* mRNA) or *Pecam1* and *Eng* (relative to the expression of *Actb* mRNA) in tumors from EL4 tumor-bearing WT, *Nlrp3* $^{-/-}$, *Casp1* $^{-/-}$, *Ctsb* $^{-/-}$ or *Il17a $^{-/-}$ mice treated with PBS or 5FU (50 mg per kg body weight). (g) As described in **Figure 5b** but using *Il17a $^{-/-}$ mice treated or not with 5FU, IL-1Ra or both. Data are representative of one out of three (a,c) or one out of two (b,d,f,g) experiments and are the mean \pm s.e.m. * P < 0.05 by Wilcoxon rank-sum test.**



DISCUSSION

Here we show that 5FU and Gem induce direct activation of the NLRP3 inflammasome through the release of cathepsin B from lysosomes, leading to secretion of IL-1 β , production of IL-17 and tumor growth. Although we previously reported a positive antitumor immune effect of 5FU caused by its capacity to deplete MDSCs⁹, 5FU also induces IL-1 β release by MDSCs. IL-1 β production could thereby restrain the beneficial effect of MDSC depletion. The *in vivo* relevance of these events may be explained by their temporal dissociation. However, we were unable to induce MDSC depletion without caspase-1 activation by modulating 5FU dose, suggesting the rationale of combining IL-1 inhibition with 5FU treatment.

In this report we demonstrate that 5FU and Gem do not induce ROS activation or potassium efflux in MDSCs, two classical activators of the inflammasome, but they do trigger NLRP3 activation through lysosome permeabilization and cathepsin B release. In addition, we show that cathepsin B induces a direct activation of Nlrp3 by binding to its LRR fragment without inducing cleavage.

Our observation underscores an atypical mode of caspase-1 activation that occurred 12 h after the stimulus induced by 5FU or Gem.

This delay is very different from those usually observed with other ligands. This result may be expected because of the requirement of 5FU to metabolize and integrate into DNA to exert its effects. In our observations, 5FU induced caspase-1 activation through lysosome destabilization. These data are in line with a previous study in which 5FU was shown to exert its cytotoxic effect through BCL2-associated X protein (Bax) activation, which is known to induce mitochondria and lysosome disruption²⁷. In our model, we found that Bax inactivation using shRNA blunted lysosome permeabilization and caspase-1 activation in MDSCs (**Supplementary Fig. 16**), thus linking this specific mechanism of 5FU cytotoxicity on MDSCs with its capacity to trigger caspase-1 activation in these cells.

Chronic inflammation is recognized as an important event in carcinogenesis and tumor progression^{28–31}. For example, chronic overactivation of the IL-1 β system³² has been considered a tumor-promoting condition, arguing in favor of IL-1 β inhibition for tumor prevention or therapy^{33–36}. In addition, IL-1 β was previously shown to negatively regulate anticancer immune responses through its capacity to induce MDSC expansion³⁷. In another model, the expression of Nlrp3 in the tumor microenvironment diminishes antitumor

immunity and vaccine efficacy by facilitating the migration of MDSCs to the tumor site³⁸, thus proposing another deleterious mechanism of action of the NLRP3 inflammasome in the context of cancer. IL-1 β was also shown to induce the generation and expansion of T_H17 cells, which could promote tumor growth by signal transducer and activator of transcription 3 (Stat3) activation in tumor cells³⁹. Stat3 then exerts proangiogenic functions that drive pathologic neoangiogenesis in tumors⁴⁰.

In sharp contrast, we have previously shown that some anticancer chemotherapeutic agents such as anthracyclines induced a specific mode of death called immunogenic cell death⁴¹. This type of tumor-cell death elicits an immune response that requires calreticulin externalization⁴², high mobility group box 1 (HMGB1) secretion⁴³, autophagy induction⁴⁴ and IL-1 β signaling for the priming of anti-cancer CD8⁺ T cells⁵, suggesting that acute inflammation triggered by chemotherapy is beneficial for anticancer responses. This discrepant result may be explained by the fact that 5FU and Gem do not induce immunogenic tumor-cell death⁹. Consequently, these drugs do not favor the cross priming of tumor antigens by dendritic cells and CD8⁺ T cell activation. In addition, the effects of IL-1 β may depend on its concentration. Although even at low concentrations IL-1 β is able to enhance IL-17 production by T cells, only high concentrations drive CD8⁺ T cell activation^{5,23}. These data may help to explain the ambiguous role of IL-1 β during tumor growth and treatment.

The specific mechanisms underlying the capacity of Gem and 5FU to target MDSCs remains unclear. We found that MDSCs have low expression of thymidylate synthase and cytidine deaminase, the rate-limiting enzymes that protect from 5FU- and Gem-induced cell death, respectively (Supplementary Fig. 17). In addition, the expression of these enzymes was inversely correlated with caspase-1 activation (data not shown). These data suggest that the specificity of 5FU and Gem in targeting MDSCs is the result of an enzymatic deficiency.

This report unravels a new mechanism of resistance to chemotherapy by highlighting the downside of two widely used anticancer cytotoxic agents, 5FU and Gem. Although these drugs induce MDSC killing and thus impede tumor-induced immunosuppression, they also mediate cathepsin B-dependent activation of the NLRP3 inflammasome. Consecutive IL-1 β release promotes a state of inflammation that enhances IL-17 production and accelerates tumor growth. As caspase-1 activation in MDSCs and IL-1 β production can also be detected in patients treated with 5FU for metastatic colon cancer, our work supports the use of inhibitors of IL-1 β or the NLRP3 inflammasome in combination with 5FU or Gem to enhance their efficacy.

METHODS

Methods and any associated references are available in the [online version of the paper](#).

Note: Supplementary information is available in the [online version of the paper](#).

ACKNOWLEDGMENTS

The authors of this work are supported by the Fondation pour la Recherche Médicale (FRM) (F.G.), the Association pour le Recherche Contre le Cancer (ARC) (F.G., G.M. and M.B.), the Ligue Nationale Contre le Cancer (F.V.), the Institut National du Cancer (INCa) (F.G.), the Ligue Régionale Contre le Cancer Comité Grand-Est (F.G., C.R. and L.A.), the Fondation de France (F.G.), the Agence Nationale de la Recherche (ANR, ANR-10-PDOC-014-01) (L.A.), the European Commission (Marie Curie Fellowship PCIG10-GA-2011-303719) (L.A.), the Ministère de l'Enseignement Supérieur et de la Recherche (M.B.), INSERM et Région Bourgogne (F.C.) and LabEx ANR-11-LABX-0021. We thank P. Schneider (Biochemistry Department, Université de Lausanne), V. Bronte (Istituto Oncologico, Padova, Italy) and T. Reinheckel (Institute of Molecular Medicine and Cell Research Freiburg, Germany) for providing essential material.

AUTHOR CONTRIBUTIONS

M.B., G.M., V.D., F.C., A.C., F.V., W.B., B.S. and C.R. performed *in vitro* experiments. M.B. and L.A. performed *in vivo* experiments. B.R., J.L.C. and J.K. provided essential materials. M.B., G.M., L.A., F.M. and F.G. designed the study and analyzed results. M.B., L.A. and F.G. wrote the paper.

COMPETING FINANCIAL INTERESTS

The authors declare no competing financial interests.

Published online at <http://www.nature.com/doi/10.1038/nm.2999>.

Reprints and permissions information is available online at <http://www.nature.com/reprints/index.html>.

- Pagès, F. *et al.* Effector memory T cells, early metastasis, and survival in colorectal cancer. *N. Engl. J. Med.* **353**, 2654–2666 (2005).
- Zhang, L. *et al.* Intratumoral T cells, recurrence, and survival in epithelial ovarian cancer. *N. Engl. J. Med.* **348**, 203–213 (2003).
- Mattarollo, S.R. *et al.* Pivotal role of innate and adaptive immunity in anthracycline chemotherapy of established tumors. *Cancer Res.* **71**, 4809–4820 (2011).
- Ménard, C., Martin, F., Apetoh, L., Bouyer, F. & Ghiringhelli, F. Cancer chemotherapy: not only a direct cytotoxic effect, but also an adjuvant for antitumor immunity. *Cancer Immunol. Immunother.* **57**, 1579–1587 (2008).
- Ghiringhelli, F. *et al.* Activation of the NLRP3 inflammasome in dendritic cells induces IL-1 β -dependent adaptive immunity against tumors. *Nat. Med.* **15**, 1170–1178 (2009).
- Sinha, P., Clements, V.K., Bunt, S.K., Albelda, S.M. & Ostrand-Rosenberg, S. Cross-talk between myeloid-derived suppressor cells and macrophages subverts tumor immunity toward a type 2 response. *J. Immunol.* **179**, 977–983 (2007).
- Le, H.K. *et al.* Gemcitabine directly inhibits myeloid derived suppressor cells in BALB/c mice bearing 4T1 mammary carcinoma and augments expansion of T cells from tumor-bearing mice. *Int. Immunopharmacol.* **9**, 900–909 (2009).
- Mundy-Bosse, B.L. *et al.* Myeloid-derived suppressor cell inhibition of the IFN response in tumor-bearing mice. *Cancer Res.* **71**, 5101–5110 (2011).
- Vincent, J. *et al.* 5-Fluorouracil selectively kills tumor-associated myeloid-derived suppressor cells resulting in enhanced T cell-dependent antitumor immunity. *Cancer Res.* **70**, 3052–3061 (2010).
- Suzuki, E., Kapoor, V., Jassar, A.S., Kaiser, L.R. & Albelda, S.M. Gemcitabine selectively eliminates splenic Gr-1⁺/CD11b⁺ myeloid suppressor cells in tumor-bearing animals and enhances antitumor immune activity. *Clin. Cancer Res.* **11**, 6713–6721 (2005).
- Apetoh, L., Vegran, F., Ladoire, S. & Ghiringhelli, F. Restoration of antitumor immunity through selective inhibition of myeloid derived suppressor cells by anticancer therapies. *Curr. Mol. Med.* **11**, 365–372 (2011).
- Ostrand-Rosenberg, S. & Sinha, P. Myeloid-derived suppressor cells: linking inflammation and cancer. *J. Immunol.* **182**, 4499–4506 (2009).
- Gabrilovich, D.I. & Nagaraj, S. Myeloid-derived suppressor cells as regulators of the immune system. *Nat. Rev. Immunol.* **9**, 162–174 (2009).
- Nagaraj, S. & Gabrilovich, D.I. Tumor escape mechanism governed by myeloid-derived suppressor cells. *Cancer Res.* **68**, 2561–2563 (2008).
- Longley, D.B., Harkin, D.P. & Johnston, P.G. 5-fluorouracil: mechanisms of action and clinical strategies. *Nat. Rev. Cancer* **3**, 330–338 (2003).
- Mini, E., Nobili, S., Caciagli, B., Landini, I. & Mazzei, T. Cellular pharmacology of gemcitabine. *Ann. Oncol.* **17** (suppl. 5), v7–v12 (2006).
- Gross, O., Thomas, C.J., Guarda, G. & Tschopp, J. The inflammasome: an integrated view. *Immunol. Rev.* **243**, 136–151 (2011).
- Pétrilli, V., Dostert, C., Muruve, D.A. & Tschopp, J. The inflammasome: a danger sensing complex triggering innate immunity. *Curr. Opin. Immunol.* **19**, 615–622 (2007).
- Buttle, D.J., Murata, M., Knight, C.G. & Barrett, A.J. CA074 methyl ester: a proinhibitor for intracellular cathepsin B. *Arch. Biochem. Biophys.* **299**, 377–380 (1992).
- Tschopp, J., Martinon, F. & Burns, K. NALPs: a novel protein family involved in inflammation. *Nat. Rev. Mol. Cell Biol.* **4**, 95–104 (2003).
- Dinarello, C.A. Why not treat human cancer with interleukin-1 blockade? *Cancer Metastasis Rev.* **29**, 317–329 (2010).
- Acosta-Rodriguez, E.V., Napolitani, G., Lanzavecchia, A. & Sallusto, F. Interleukins 1 β and 6 but not transforming growth factor- β are essential for the differentiation of interleukin 17-producing human T helper cells. *Nat. Immunol.* **8**, 942–949 (2007).
- Chung, Y. *et al.* Critical regulation of early Th17 cell differentiation by interleukin-1 signaling. *Immunity* **30**, 576–587 (2009).
- Qin, H. *et al.* TGF- β promotes Th17 cell development through inhibition of SOCS3. *J. Immunol.* **183**, 97–105 (2009).
- He, D. *et al.* IL-17 promotes tumor development through the induction of tumor promoting microenvironments at tumor sites and myeloid-derived suppressor cells. *J. Immunol.* **184**, 2281–2288 (2010).
- Kujawski, M. *et al.* Stat3 mediates myeloid cell-dependent tumor angiogenesis in mice. *J. Clin. Invest.* **118**, 3367–3377 (2008).
- Wang, C. & Youle, R.J. Predominant requirement of Bax for apoptosis in HCT116 cells is determined by Mcl-1's inhibitory effect on Bak. *Oncogene* **31**, 3177–3189 (2012).

28. Carmi, Y. *et al.* Microenvironment-derived IL-1 and IL-17 interact in the control of lung metastasis. *J. Immunol.* **186**, 3462–3471 (2011).
29. Apte, R.N. & Voronov, E. Is interleukin-1 a good or bad 'guy' in tumor immunobiology and immunotherapy? *Immunol. Rev.* **222**, 222–241 (2008).
30. Grivennikov, S.I., Greten, F.R. & Karin, M. Immunity, inflammation, and cancer. *Cell* **140**, 883–899 (2010).
31. Li, N., Grivennikov, S.I. & Karin, M. The unholy trinity: inflammation, cytokines, and STAT3 shape the cancer microenvironment. *Cancer Cell* **19**, 429–431 (2011).
32. Krelm, Y. *et al.* Interleukin-1 β -driven inflammation promotes the development and invasiveness of chemical carcinogen-induced tumors. *Cancer Res.* **67**, 1062–1071 (2007).
33. Hagemann, T., Balkwill, F. & Lawrence, T. Inflammation and cancer: a double-edged sword. *Cancer Cell* **12**, 300–301 (2007).
34. Greten, F.R. *et al.* IKK β links inflammation and tumorigenesis in a mouse model of colitis-associated cancer. *Cell* **118**, 285–296 (2004).
35. Naugler, W.E. *et al.* Gender disparity in liver cancer due to sex differences in MyD88-dependent IL-6 production. *Science* **317**, 121–124 (2007).
36. Balkwill, F., Charles, K.A. & Mantovani, A. Smoldering and polarized inflammation in the initiation and promotion of malignant disease. *Cancer Cell* **7**, 211–217 (2005).
37. Bunt, S.K. *et al.* Reduced inflammation in the tumor microenvironment delays the accumulation of myeloid-derived suppressor cells and limits tumor progression. *Cancer Res.* **67**, 10019–10026 (2007).
38. van Deventer, H.W. *et al.* The inflammasome component NLRP3 impairs antitumor vaccine by enhancing the accumulation of tumor-associated myeloid-derived suppressor cells. *Cancer Res.* **70**, 10161–10169 (2010).
39. Wang, L. *et al.* IL-17 can promote tumor growth through an IL-6–Stat3 signaling pathway. *J. Exp. Med.* **206**, 1457–1464 (2009).
40. Numasaki, M. *et al.* Interleukin-17 promotes angiogenesis and tumor growth. *Blood* **101**, 2620–2627 (2003).
41. Zitvogel, L., Apetoh, L., Ghiringhelli, F. & Kroemer, G. Immunological aspects of cancer chemotherapy. *Nat. Rev. Immunol.* **8**, 59–73 (2008).
42. Obeid, M. *et al.* Calreticulin exposure dictates the immunogenicity of cancer cell death. *Nat. Med.* **13**, 54–61 (2007).
43. Apetoh, L. *et al.* Toll-like receptor 4–dependent contribution of the immune system to anticancer chemotherapy and radiotherapy. *Nat. Med.* **13**, 1050–1059 (2007).
44. Michaud, M. *et al.* Autophagy-dependent anticancer immune responses induced by chemotherapeutic agents in mice. *Science* **334**, 1573–1577 (2011).

ONLINE METHODS

Mice. For all experiments, only female mice were used. *Nlrp3*^{-/-} transgenic mice were provided by J.-L.C. *P2rx7*^{-/-} transgenic mice were obtained from J.K. *Casp1*^{-/-}, *Il17a*^{-/-}, *Il1r1*^{-/-} and ROR- γ -GFP mice were given by B.R., and *Ctsb*^{-/-} mice were provided by T. Reinheckel. All mice were on a C57BL/6 background. Female C57BL/6 and BALB/c mice (aged 6–8 weeks) were obtained from the Centre d'élevage Janvier and Charles River Laboratories.

Cell lines. MSC-2 is an immortalized MDSC cell line obtained from BALB/c Gr-1⁺ splenocytes and was obtained here from V. Bronte (Istituto Oncologico, Padova, Italy). EL4 thymoma cells, LLC cells and B16F10 melanoma cancer cells (all syngenic from C57BL/6 mice), 4T1 mammary adenocarcinoma cancer cells (syngenic from BALB/c mice) and MSC-2 cells were cultured at 37 °C under 5% CO₂ in RPMI 1640 with 10% (v/v) FCS supplemented with sodium pyruvate, penicillin and streptomycin and 4 mM 4-(2-hydroxyethyl)-1-piperazine-ethanesulfonic acid (HEPES).

Chemotherapeutic drugs. For *in vitro* experiments, unless otherwise stated, cells were treated for 24 h with 5FU (Sanofi-Aventis) at 1 μ M, Gem (Lilly France) at 27 nM or oxaliplatin (Teva) at 2.5 μ M. For drug screening, Deticene (Sanofi-Aventis) was used at 430 μ M, paclitaxel (Bristol-Myers Squibb) at 175 nM, mitomycin C (Sigma-Aldrich) at 3 μ M and doxorubicin (Pfizer) at 73 nM.

In vivo treatments. To induce tumor formation, 10⁶ EL4, 3 \times 10⁵ B16F10, 10⁵ 4T1 or 3 \times 10⁵ LLC cells were injected subcutaneously into mice. All experiments were carried out in accordance with guidelines prescribed by the Ethics Committee at the University of Burgundy.

EL4 tumor-bearing mice received a single injection of 5FU at 50 mg per kg body weight or Gem at 120 mg per kg body weight 10 d after tumor-cell injection (tumor size, 100–120 mm²). B16F10 tumor-bearing mice were treated with three injections of 5FU at 50 mg per kg body weight at days 5, 7 and 9 after tumor-cell injection. 4T1 and LLC tumor-bearing mice received two injections of 5FU at 50 mg per kg body weight at days 5 and 7. For each model, we chose the minimal number of 5FU injections that would induce a delay in tumor growth in wild-type mice. Thirty micrograms of IL-1Ra (Kineret from Biovitrum) were injected three times a week beginning with the chemotherapeutic treatment at day 10. All drugs were administered intraperitoneally.

To deplete CD4 or CD8 cells, mice were injected with 250 μ g of CD4-specific (GK 1.5) or CD8-antibodies (2.43) antibodies (obtained from BioXcell) at days 0 and 3 after chemotherapeutic treatment. To deplete MDSCs, mice were injected with 200 μ g of Gr-1-specific monoclonal antibody (BE0075) from BioXcell at days -2 and -1 before 5FU injection.

Reagents. Cytochalasin D (C8273), oxi ATP (A 6779), CaCl₂ (C3881), bafilomycin A1 (B1793), LPS and ATP (A7699) were all purchased from Sigma-Aldrich (St. Louis, MO, USA). *N*-acetylcysteine was from Zambon, apocynin (17838) was bought from MERCK, and KCl was purchased from PROAMP. All tissue culture reagents were bought from Lonza.

Determination of caspase-1 activity. To assess caspase-1 activity, the FAM-YVAD-FMK fluorescent probe (Immunochemistry Technologies Bloomington) binding to cleaved caspase-1 was used according to the manufacturer's instructions. Briefly, 4 \times 10⁶ cells per ml were cultured for 45 min in the presence of the substrate, and cells were subsequently washed and analyzed by flow cytometry in the presence of DAPI from Sigma-Aldrich to exclude necrotic cells.

ELISA. Cell culture supernatants were assayed for mouse IL-1 β (R&D Systems), IL-17a (Biolegend) IFN- γ or IL-4 (BD Biosciences, Franklin Lakes, NJ, USA). Human sera were tested for IL-1 β (BD Biosciences and R&D Systems) and IL-17 (Biolegend) according to the manufacturers' instructions.

Flow cytometry analyses. Fluorescence-activated cell sorting (FACS) analyses on mouse cells were performed using phycoerythrin-cyanine 7 (PE-Cy7)-conjugated antibodies to Gr-1 (RB6-8C5 from ebioscience, San Diego, CA, USA), PE-conjugated antibodies to CD11c (N418 from ebioscience), Alexa Fluor 700-conjugated F4/80 (BM8 from Biolegend), allophycocyanin (APC)-conju-

gated antibodies to CD11b (M1/70 from abcam, Paris, France), DAPI, fluorescein isothiocyanate (FITC)-conjugated annexin V (from BD Pharmingen) and lysotracker (DND-26 from Invitrogen). All antibodies were diluted to 1:100.

For human cell labeling, we used APC-conjugated antibodies to CD33 (WM53), PE-conjugated antibodies to CD14 (M5E2) and peridin-chlorophyll-protein complex (PercP)-conjugated antibodies to HLA-DR (L243), all purchased from BD Pharmingen and used according to the manufacturer's protocol.

All acquisitions were performed with a BD LSR-II cytometer equipped with BD FACSDiva software (BD biosciences), and all data were analyzed with FlowJo software.

Immunoblot analysis. Protein extracts were prepared by lysing cells in boiling buffer (1% SDS, 1 mM sodium vanadate and 10 mM Tris, pH 7.4) in the presence of complete protease inhibitors (Roche diagnostics) for 10 min at 4 °C. Viscosity of the samples was reduced by sonication. Protein concentration was measured using the Bio-Rad DC protein assay kit. Protein lysates were incubated in loading buffer (125 mM Tris-HCl, pH 6.8, 10% β -mercaptoethanol, 4.6% SDS, 20% glycerol and 0.003% bromophenol blue), heated at 95 °C for 5 min and then separated by SDS-PAGE and electroblotted to a nitrocellulose membrane (Schleicher and Schuell). After incubation for 2 h at room temperature with 5% nonfat milk or BSA in Tris-buffered saline and 0.1% Tween 20 (TBS-Tween), membranes were incubated overnight with primary antibody diluted in 5% nonfat milk or BSA in TBS-Tween, washed, incubated with secondary antibody for 30 min at room temperature and washed again before analysis with luminol reagent (Santa Cruz Biotechnologies).

Rabbit polyclonal antibody to mouse caspase-1 was purchased from Invitrogen (AHZ0082, 1:1,000) or Santa Cruz (M-20, 1:200). Rat monoclonal antibody to mouse IL-1 β was obtained from R&D Systems (166926, 1:500). Mouse monoclonal antibodies to the following were used: β -actin (A1978, 1:5,000) and VSV-G (V4888, 1:1,000) (Sigma-Aldrich) and Nlrp3 (Cryo2, 1:1,000, Enzo Life Sciences). Goat polyclonal antibody to cathepsin B (S-12, 1:200) was obtained from Santa Cruz.

Immunoblot analysis of mice serum. Two-hundred microliters of mouse serum was immunoprecipitated using rat monoclonal antibody to mouse IL-1 β (166926, 1:125, R&D Systems) and analyzed using immunoblot analysis.

Cell proliferation assay. For the cell proliferation assay, 4T1, B16, LLC or EL4 cells were seeded at 1 \times 10⁴ cells per well in a 96-well plate. To assess the impact of IL-1 β on tumor-cell survival after 5FU treatment, cells were treated for 24 h with IL-1 β (200 pg ml⁻¹) before receiving 5FU. Two days after 5FU treatment, cell survival was determined by crystal violet staining for 4T1, B16 and LLC cells and flow cytometry using annexin V and DAPI staining for EL4 cells.

Confocal microscopy. Cells were cultured on glass in complete medium. They were fixed and permeabilized using BD Cytofix/Cytoperm buffer (BD bioscience) and saturated with BD Perm/Wash containing 5% BSA. The primary antibodies used were rat antibodies to mouse CD107a (SC71488, 4 μ g ml⁻¹, Santa Cruz Biotechnology) and goat antibodies to mouse cathepsin B (SC6493, 4 μ g ml⁻¹, Santa Cruz), and the secondary antibodies used were antibodies to rat Alexa 488 (1:1,000) and antibodies to goat Alexa 594 (1:1,000) from Invitrogen. Samples were observed with a LEICA TCS SP2 microscope (Leica microsystem SAS). Pictures were merged using ImageJ.

Recombinant proteins. Recombinant human NLRP3 protein (H00114548-P01) was obtained from Abnova, and recombinant human cathepsin B (953-CY) and mouse cathepsin B (965-CY) were purchased from R&D Systems.

To synthesize recombinant mouse Nlrp3 and VSV-tagged recombinant mouse Nlrp3 deleted in the PYD or the NACHT or LRR domain, we used the TNT T7 quick-coupled transcription/translation system from Promega according to the manufacturer's instructions.

Plasmid constructs. The sequence coding for *Nlrp3* was inserted in the pCR3-VSV N-ter plasmid (kind gift from P. Schneider). *Nlrp3* deleted in the PYD or the NACHT or LRR domain were generated by site-directed mutagenesis with

the GeneTailor mutagenesis system (Invitrogen). The sequences of the oligonucleotides used are listed in **Supplementary Table 2**.

Knockdown of *Nlrp3*, *Ctsb* or *Bax* expression in MSC-2 cells. MSC-2 cells were transduced with MISSION Lentiviral Transduction Particles (Sigma-Aldrich) to silence *Nlrp3*, *Ctsb* or *Bax* or with negative control particles according to the manufacturer's instructions. Briefly, 1.6×10^4 cells were seeded in 96-well plates, and the next day, lentiviral particles (multiplicity of infection tested between 0.5 and 10) were added in the presence of $8 \mu\text{g ml}^{-1}$ of hexadimethrine bromide (Sigma-Aldrich) for 20 h. Then the medium was removed and replaced by fresh medium containing $3 \mu\text{g ml}^{-1}$ of puromycin (Sigma-Aldrich) every 3 d until obtaining resistant cells. Resistant cells transduced with control shRNA particles and others transduced with shRNA specific for *Nlrp3*, *Ctsb* or *Bax* were obtained. Downregulation of *Nlrp3*, cathepsin B and *Bax* was checked by western blotting.

Determination of cathepsin B activity. To assess cathepsin B activity, 2×10^5 cells were incubated in the presence of a fluorogenic cathepsin B substrate (100 μM , 219392, EMD chemicals) for 30 min at 37 °C. Fluorometry was then measured at 460 nm using a Wallac 1440 Victor2 luminometer (PerkinElmer).

Experiments with Human PBMCs. For *in vitro* experiments, 2.5×10^6 PBMCs from patients with cancer were cultured in 200 μl of RPMI with PBS or 5FU (40 μM) in the presence or absence of CA074Me at 33 μM (205531 from Calbiochem) for 2 d. Caspase-1 activation in HLA DR⁺CD14⁺CD33⁺ MDSCs was assessed using flow cytometry.

For *in vivo* experiments, PBMCs and sera from patients with colon cancer were obtained before and 1 d after 5FU treatment. Caspase-1 activation was determined in HLA DR⁺CD14⁺CD33⁺ MDSCs. Experiments were approved by the local ethical committee (Institutional Review Board of the Centre Georges Francois Leclerc).

Surface plasmon resonance analysis. The design and fabrication of homemade chips compatible with surface plasmon resonance was performed as previously published with the help of the MIMENTO technological platform (Besançon, France)⁴⁵.

Biacore experiments were performed with the Biacore 2000 apparatus at 25 °C with a flow rate of 2–30 $\mu\text{l min}^{-1}$. Human cathepsin B and rat serum albumin (both at 15 $\mu\text{g ml}^{-1}$) were immobilized on chemically activated self-assembly monolayers of 11-mercapto-1-undecanol (11-MUOH) and 16-mercapto-1-hexadecanoic acid (16-MHA) (97/3 by mole). Real-time monitoring allowed the control of 10 femtomoles per mm^2 of immobilized proteins in each experiment. Human NLRP3 was injected at 10 nM in PBS buffer according to the Kinject procedure (association time, 2 min; dissociation time, 3 min).

Coculture of naive T cells with MDSCs. Two days after PBS or 5FU treatment *in vivo*, splenic MDSCs from EL4 tumor-bearing mice (tumor size, 80–100 mm^2) and splenic CD4⁺CD62L⁺ naive T cells from naive mice were sorted by flow cytometry with a BD ARIA cytometer equipped with BD FACSDiva software (BD biosciences). Two-hundred thousand naive T cells were cultured with 2×10^5 MDSCs in RPMI in the presence of antibodies to CD3 (5 $\mu\text{g ml}^{-1}$) and CD28 (5 $\mu\text{g ml}^{-1}$) for 3 d. IL-17a production was assessed by ELISA.

Quantitative PCR analysis. Total RNA from T cells was extracted using TRIzol (Invitrogen). One hundred to three hundred nanograms of RNA were reverse transcribed into complementary DNA (cDNA) using Moloney murine leukemia virus (M-MLV) reverse transcriptase, random primers and RNaseOUT inhibitor (Invitrogen). cDNAs were quantified by real-time PCR using a SYBR Green Real-time PCR kit (Applied Biosystems) on a Fast7500 detection system (Applied biosystems). Relative mRNA levels were determined using the ΔCt method. Values were expressed relative to CD3. The sequences of the oligonucleotides used are listed in **Supplementary Table 2**.

***In vitro* T cell differentiation.** Naive CD4⁺ T cells (CD4⁺CD62L^{hi}) or naive CD8⁺ T cells (CD8a⁺) were isolated from spleens and lymph nodes of C57BL/6 wild-type mice using magnetic beads from Miltenyi Biotec. Naive CD4⁺ T cells were stimulated with plate-bound antibodies to CD3 (145-2C11, 10 $\mu\text{g ml}^{-1}$) and CD28 (PV-1, 10 $\mu\text{g ml}^{-1}$) in the presence of either no cytokines or IL-6 (20 ng ml^{-1}), TGF- β (2 ng ml^{-1}), antibodies to IFN- γ (10 $\mu\text{g ml}^{-1}$) and antibodies to IL-4 (10 $\mu\text{g ml}^{-1}$) to obtain T_{H0} and T_{H17} cells, respectively. Naive CD8⁺ T cells were stimulated with plate-bound antibodies to CD3 and CD28, and IL-12 (10 ng ml^{-1}) was added to obtain Tc1 cells. Mouse IL-1 β (401-ML), IL-6 (406-ML), IL-12 (419-ML) and TGF- β (100-B) were all purchased from R&D Systems. Antibodies to IL-4 (1B11) and IFN- γ (XMG1.2) were obtained from BioXcell.

Bone marrow-derived dendritic cells. Bone marrow-derived dendritic cells were propagated in Iscove's Modified Dulbecco's Medium (IMDM) (Sigma-Aldrich) supplemented with penicillin (100 UI ml^{-1} ; Gibco), streptomycin (100 $\mu\text{g ml}^{-1}$; Gibco), L-glutamine (Gibco), 2-mercaptoethanol (50 μM ; Sigma), 10% heat-inactivated endotoxin-free FCS (Gibco) and granulocyte-macrophage colony-stimulating factor (GM-CSF) (20 ng ml^{-1} ; R&D Systems). Dendritic cells were used between days 10 and 12 when the proportion of dendritic cells within the culture was above 80%, as determined by coexpression of CD11c and MHC class II antigens.

Isolation of mouse peritoneal macrophages. Peritoneal cells were isolated by lavage with 4 ml of ice-cold PBS containing NaCl (150 mM; Sigma-Aldrich). Cells were seeded in 24-well plates in culture medium. Twenty-four hours later, the supernatant was discarded, and the adherent cells were regarded as macrophages.

Statistical analyses. Results are shown as means \pm s.e.m., and comparisons of datasets were performed using unpaired Student's *t* test (test group compared to control group). For human experiments, paired *t* test was used to compare samples from the same patients before and after 24 h of 5FU treatment, and Wilcoxon matched-pairs signed-rank test was used to compare samples from the same patients before and 14 d after 5FU treatment. Differences in survival in the tumor growth experiments were assessed using Fisher's exact test. We performed statistical calculations with GraphPad Prism 5. All *P* values were two tailed. *P* < 0.05 was considered statistically significant for all experiments.

45. Boireau, W., Rouleau, A., Lucchi, G. & Ducoroy, P. Revisited BIA-MS combination: entire "on-a-chip" processing leading to the proteins identification at low femtomole to sub-femtomole levels. *Biosens. Bioelectron.* **24**, 1121–1127 (2009).